Chapter 95
Analysis of Ship Shaft Bending Vibration Characteristics Based on Bearing Oil Film Stiffness

Shuqing Liu, Rui Huo, Yuanbo Li, and Chuangye Li

Abstract Propulsion shafting plays an important role in the overall structure of naval ships. The control effect of shafting vibration determines the safety performance of the ship to a great extent. The dynamic characteristics of the sliding bearing distributed on the shaft, especially the stiffness, have a significant influence on the vibration transmission characteristics of the propulsion shafting. The study of the influence of bearing stiffness characteristics on the coupling vibration of propulsion shafting and hull is beneficial to promote the optimal design of shafting and improve the safety performance of ships. In this article, according to the general structure of ship propulsion shafting, the theoretical model of ship-shaft coupling system bending vibration is established, and the calculation model of average energy input of each shaft section is deduced. The oil film stiffness characteristics of various bearings on the stern drive shaft are simulated and analyzed. The results show that the bearing liquid film stiffness is proportional to the shaft speed and inversely proportional to the main resonance peak frequency. The stiffness of bearing liquid film is proportional to the strength of low frequency vibration energy transmission dissipation, but has little effect on the dissipation process of high frequency vibration energy transmission.

Keywords Bearing oil film rigidity · Ship shafting · Bending vibration characteristics · Average energy input

95.1 Introduction

Thrust bearing is a key component of the Marine propulsion system. It transmits thrust from the propeller to the hull [1]. The modern ships pay more attention to

S. Liu · R. Huo (✉) · Y. Li · C. Li
School of Mechanical Engineering, Shandong University, Ji'nan 250061, China
e-mail: huorui@sdu.edu.cn

Key Laboarotory of High Efficiency and Clean Mechanical Manufacture, Shandong University, Ministry of Education, Ji'nan 250061, China

Y. Li
92143 force of PLA, San'ya 572000, China

J. Tan (ed.), *Advances in Mechanical Design*, Mechanisms and Machine Science 111,
https://doi.org/10.1007/978-981-16-7381-8_95

the large size and long voyage ability, at the same time, Military ships also need to have high-speed and high-maneuverability capabilities, so the requirements for bearing performance are becoming more stringent [2]. The research on the vibration of the propulsion shafting has always been a hot issue in the research and design of ships [3]. The stiffness of bearing liquid film is one of the key factors affecting the vibration characteristics in ship shafting. In most of the previous researches on shafting vibration, the stiffness of bearing liquid film is often simply defined as an ideal spring with fixed dynamic characteristics.

Studies have shown that the lubrication characteristics of each bearing in the propulsion shaft system have a more great influence on the bending vibration of the system than on the longitudinal vibration [4, 5]. Based on the general structure of the ship's propulsion shafting system, this paper conducts dynamic analysis, modeling analysis, and establishes the flexural vibration model of the propulsion shaft system-hull coupling system and the average energy calculation model. Use ANSYS to analyze the oil film stiffness characteristics of each bearing on the stern drive shaft; then the calculation results were substituted into the bending vibration energy transfer average power calculation model for effect analysis.

95.2 Shaft Bending Vibration Modeling and Power Flow Calculation

Firstly, based on the assumption that the dynamic characteristics of each bearing are invariable, Modeling the bending vibration of shafting system and deriving the average energy input formula. To streamline the modeling process, in Sect. 95.2.1 just list the differential equation after the Fourier transform. In Sect. 95.2.2, the concepts of complex stiffness and complex wave number are introduced to express the average power of energy input of propeller excitation.

95.2.1 Mode Building and Solving

As shown in Fig. 95.1, consider the axis as a simply supported boundary condition. Research has shown that pedestal bearing, stern front bearing, stern intermediate bearing and rear stern bearing's radial restraint is very large, while Air–tire clutch, elastic coupling and thrust bearing's radial constraints are relatively small [6].

Figure 95.2 is the schematic diagram of vibration energy transfer relationship of tail shaft L_2, regard the contact among the bearings, the main shaft and the hull mounting base as point contact, and the dynamic characteristics of each bearing are fixed. F_p is the lateral excitation force input by the drive axial propeller, J_P is the moment of inertia of the ship's propeller around the main axis, The stiffness parameters of thrust bearing, front stern, middle stern, and rear stern bearings are

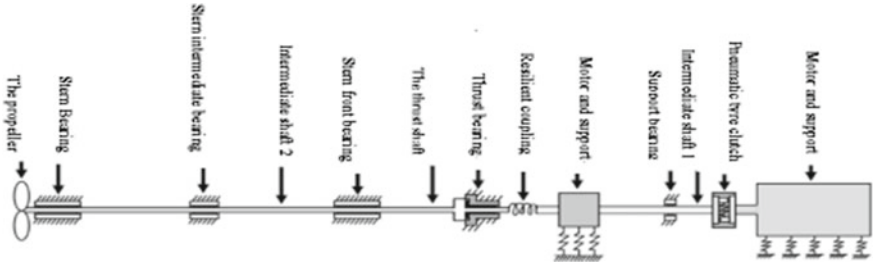

Fig. 95.1 Propulsion shaft structure diagram

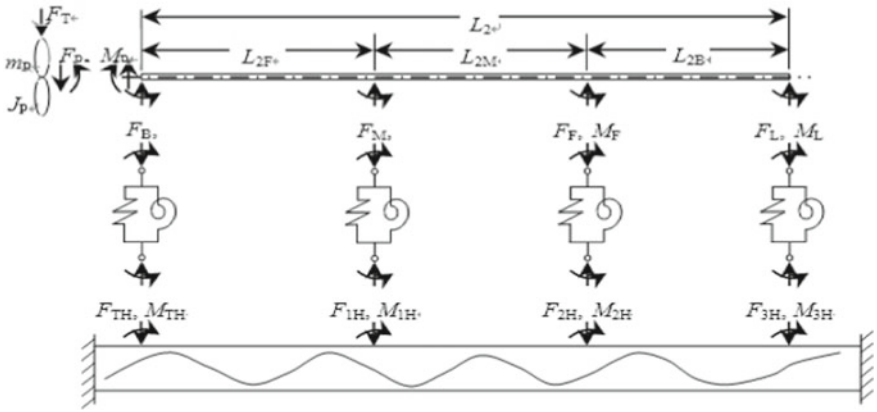

Fig. 95.2 Schematic diagram of energy transmission of shafting bending vibration

represented by k_T, k_1, k_2 and k_3 respectively; shafts from thrust bearing to front stern bearing, front stern bearing to middle stern bearing, middle stern bearing to rear stern bearing The segment distance is represented by l_{2F}, l_{2M} and l_{2B} respectively, $\tilde{F}_{MP}$ is the shear force formed by the propeller on the drive shaft, and M_P is the bending moment.

Set the vertical upward direction as the positive direction, take the propeller as the research object, and then write the equation and do the Fourier transform as follows.

$$-\omega^2 J_P \Theta_P + j\omega c_P \Theta_P = \underline{\tilde{M}}_P \tag{95.1}$$

$$\omega^2 m_P W_P - j\omega c_{P3} W_P = \underline{\tilde{F}}_P + \underline{\tilde{F}}_{MP} \tag{95.2}$$

$$-\rho A W(x,\omega) + (EI) W_{xxxx}(x,\omega) = 0 \tag{95.3}$$

$$\begin{cases} W(x_2,\omega) = W_{2\mathrm{B}}(x,\omega)\ (0 \le x \le l_{2\mathrm{B}}) \\ W(x,\omega) = W_{2\mathrm{M}}(x,\omega)\ (l_{2\mathrm{B}} \le x \le l_{2\mathrm{B}} + l_{2\mathrm{M}}) \\ W(x,\omega) = W_{2\mathrm{M}}(x,\omega)\ (l_{2\mathrm{B}} + l_{2\mathrm{M}} \le x \le L_2) \end{cases} \tag{95.4}$$

Define ${\lambda_{\mathrm{B}}}^4 = \rho S\omega^2/(EI)$, where λ_{B} is wave number,$\lambda_{2\mathrm{B}}$,$\lambda_{2\mathrm{M}}$,$\lambda_{2\mathrm{F}}$ as wave number at each axis. Equation (95.3) has a general solution:

$$W(x,\omega) = A \cdot \exp(-\mathrm{j}l_{\mathrm{B}}x) + B \cdot \exp(-l_{\mathrm{B}}x) + C \cdot \exp(\mathrm{j}l_{\mathrm{B}}x) + D \cdot \exp(l_{\mathrm{B}})$$

Contrast formula (95.4), there are formula 95.5.

$$\begin{cases} W_{2B} = \left[\exp(-j\lambda_{2B}x)\ \exp(-\lambda_{2B}x)\right]\begin{bmatrix} A_{2B} \\ B_{2B} \end{bmatrix} \\ \qquad + \left[\exp(j\lambda_{2B}x)\ \exp(\lambda_{2B}x)\right]\begin{bmatrix} C_{2B} \\ D_{2B} \end{bmatrix} 0 \le x \le l_{2B} \\ W_{2M} = \left[\exp(-j\lambda_{2M}x)\exp(-\lambda_{2M}x)\right]\begin{bmatrix} A_{2M} \\ B_{2M} \end{bmatrix} \\ \qquad + \left[\exp(j\lambda_{2M}x)\ \exp(\lambda_{2M}x)\right]\begin{bmatrix} C_{2M} \\ D_{2M} \end{bmatrix} l_{2B} \le x \le l_{2B} + l_{2M} \\ W_{2F} = \left[\exp(-j\lambda_{2F}x)\exp(-\lambda_{2F}x)\right]\begin{bmatrix} A_{2F} \\ B_{2F} \end{bmatrix} \\ \qquad + \left[\exp(j\lambda_{2F}x)\ \exp(\lambda_{2F}x)\right]\begin{bmatrix} C_{2F} \\ D_{2F} \end{bmatrix} l_{2B} \le l_{2M} \le x \le L_2 \end{cases} \tag{95.5}$$

Set Λ ij as a functional expression about the free vibration frequency of the system, it can be obtained through the process of deriving the vibration response between the sub-bearing and the main shaft, and finally get the matrix Eq. 95.6.

Solve the $\alpha_{2\mathrm{B}+}$, $\alpha_{2\mathrm{B}}{}^{-}$, $\alpha_{2\mathrm{M}}{}^{+}$, $\alpha_{2\mathrm{M}}{}^{-}$, $\alpha_{2\mathrm{F}}{}^{+}$ and $\alpha_{2\mathrm{F}}{}^{-}$ in the formula.

$$\begin{bmatrix} \Lambda_{11} & \Lambda_{12} & \Lambda_{13} & \Lambda_{14} & \Lambda_{15} & \Lambda_{16} \\ \Lambda_{21} & \Lambda_{22} & \Lambda_{23} & \Lambda_{24} & \mathbf{O} & \mathbf{O} \\ \Lambda_{31} & \Lambda_{32} & \Lambda_{33} & \Lambda_{34} & \Lambda_{35} & \Lambda_{36} \\ \mathbf{O} & \mathbf{O} & \Lambda_{43} & \Lambda_{44} & \Lambda_{45} & \Lambda_{46} \\ \Lambda_{51} & \Lambda_{52} & \Lambda_{53} & \Lambda_{54} & \Lambda_{55} & \Lambda_{56} \\ \Lambda_{61} & \Lambda_{62} & \Lambda_{63} & \Lambda_{64} & \Lambda_{65} & \Lambda_{66} \end{bmatrix} \begin{bmatrix} \alpha_{2\mathrm{B}}^{+} \\ \alpha_{2\mathrm{B}}^{-} \\ \alpha_{2\mathrm{M}}^{+} \\ \alpha_{2\mathrm{M}}^{-} \\ \alpha_{2\mathrm{F}}^{+} \\ \alpha_{2\mathrm{F}}^{-} \end{bmatrix} = \Lambda \begin{bmatrix} \alpha_{2\mathrm{B}}^{+} \\ \alpha_{2\mathrm{B}}^{-} \\ \alpha_{2\mathrm{M}}^{+} \\ \alpha_{2\mathrm{M}}^{-} \\ \alpha_{2\mathrm{F}}^{+} \\ \alpha_{2\mathrm{F}}^{-} \end{bmatrix} = \begin{bmatrix} \mathbf{F}_{MP} \\ 0 \\ 0 \\ 0 \\ 0 \\ 0 \end{bmatrix} \tag{95.6}$$

$$e_{2\mathrm{B}}^{+} = \mathrm{diag}[\exp(-\mathrm{j}l_{2\mathrm{B}}x), \exp(-l_{2\mathrm{B}}x)\big], \alpha_{2\mathrm{M}}^{+} = \big[A_{2\mathrm{M}}, B_{2\mathrm{M}}\big]^{\mathrm{T}},$$
$$e_{2\mathrm{B}}^{-} = \mathrm{diag}[\exp(\mathrm{j}l_{2\mathrm{B}}x),\ \exp(l_{2\mathrm{B}}x)], \alpha_{2\mathrm{M}}^{-} = [C_{2\mathrm{M}}, D_{\mathrm{FM}}]^{\mathrm{T}},$$
$$e_{2\mathrm{M}}^{+} = \mathrm{diag}[\exp(-\mathrm{j}l_{2\mathrm{M}}x),\ \exp(-l_{2\mathrm{M}}x)\big], \alpha_{2\mathrm{F}}^{+} = \big[A_{2\mathrm{F}}, B_{2\mathrm{F}}\big]^{\mathrm{T}},$$
$$e_{2\mathrm{M}}^{-} = \mathrm{diag}[\exp(\mathrm{j}l_{2\mathrm{M}}x), \exp(l_{2\mathrm{M}}x)], \alpha_{2\mathrm{F}}^{-} = [C_{2\mathrm{F}}, D_{2\mathrm{F}}]^{\mathrm{T}},$$
$$e_{2\mathrm{F}}^{+} = \mathrm{diag}[\exp(-\mathrm{j}l_{2\mathrm{F}}x),\ \exp(-l_{2\mathrm{F}}x)],$$
$$e_{2\mathrm{F}}^{-} = \mathrm{diag}[\exp(\mathrm{j}l_{2\mathrm{F}}x), \exp(l_{2\mathrm{F}}x)].$$

$$\mathbf{f}_{2\mathrm{B}}^{+} = (EI)_{2B}\lambda_{2B}^{2}\begin{bmatrix} -1 & 1 \\ \mathrm{j}\lambda_{2B} & -\lambda_{2B} \end{bmatrix}, \mathbf{W}_{2\mathrm{B}}^{+} = \begin{bmatrix} -1 & 1 \\ -\mathrm{j}\lambda_{2B} & -\lambda_{2B} \end{bmatrix}$$
$$\mathbf{f}_{2\mathrm{B}}^{-} = (EI)_{2\mathrm{B}}\lambda_{2\mathrm{B}}^{2}\begin{bmatrix} -1 & 1 \\ -\mathrm{j}\lambda_{2B} & \lambda_{2B} \end{bmatrix}, \mathbf{W}_{2\mathrm{B}}^{-} = \begin{bmatrix} 1 & 1 \\ \mathrm{j}\lambda_{2B} & \lambda_{2B} \end{bmatrix}$$
$$\mathbf{f}_{2\mathrm{M}}^{+} = (EI)_{2\mathrm{M}}\lambda_{2\mathrm{M}}^{2}\begin{bmatrix} -1 & 1 \\ \mathrm{j}\lambda_{2\mathrm{M}} & -\lambda_{2\mathrm{M}} \end{bmatrix}, \mathbf{W}_{2\mathrm{M}}^{+} = \begin{bmatrix} 1 & 1 \\ -\mathrm{j}\lambda_{2\mathrm{M}} & -\lambda_{2\mathrm{M}} \end{bmatrix}$$
$$\mathbf{f}_{2\mathrm{M}}^{-} = (EI)_{2\mathrm{M}}\lambda_{2\mathrm{M}}^{2}\begin{bmatrix} -1 & 1 \\ -\mathrm{j}\lambda_{2\mathrm{M}} & -\lambda_{2\mathrm{M}} \end{bmatrix}, \mathbf{W}_{2\mathrm{M}}^{-} = \begin{bmatrix} 1 & 1 \\ \mathrm{j}\lambda_{2\mathrm{M}} & \lambda_{2\mathrm{M}} \end{bmatrix}$$
$$\mathbf{f}_{2\mathrm{F}}^{+} = (EI)_{2\mathrm{F}}\lambda_{2\mathrm{F}}^{2}\begin{bmatrix} -1 & 1 \\ -\mathrm{j}\lambda_{2\mathrm{F}} & -\lambda_{2\mathrm{F}} \end{bmatrix}, \mathbf{W}_{2\mathrm{F}}^{+} = \begin{bmatrix} 1 & 1 \\ -\mathrm{j}\lambda_{2\mathrm{F}} & -\lambda_{2\mathrm{M}} \end{bmatrix}$$
$$\mathbf{f}_{2\mathrm{F}}^{-} = (EI)_{2\mathrm{F}}\lambda_{2\mathrm{F}}^{2}\begin{bmatrix} -1 & 1 \\ -\mathrm{j}\lambda_{2\mathrm{F}} & \lambda_{2\mathrm{F}} \end{bmatrix}, \mathbf{W}_{2\mathrm{F}}^{-} = \begin{bmatrix} 1 & 1 \\ \mathrm{j}\lambda_{2\mathrm{F}} & \lambda_{2\mathrm{F}} \end{bmatrix}$$
$$\mathbf{O} = \begin{bmatrix} 0\ 0 \\ 0\ 0 \end{bmatrix}, \mathrm{o} = \begin{bmatrix} 0 \\ 0 \end{bmatrix}$$

$$\mathbf{\Lambda}_{11} = \boldsymbol{f}_{2\mathrm{B}}^{+} + (\omega^2 J_{\mathrm{P2}} - \mathrm{j}\omega c_{\mathrm{P2}} + \boldsymbol{R}_2 z_{\mathrm{F11}})\boldsymbol{w}_{2\mathrm{B}}^{+} + \boldsymbol{R}_2 z_{\mathrm{F12}}\boldsymbol{w}_{2\mathrm{B}}^{+}\boldsymbol{e}_{2\mathrm{B}}^{+}(l_{2\mathrm{B}}),$$
$$\mathbf{\Lambda}_{12} = \boldsymbol{f}_{2\mathrm{B}}^{-} - (\omega^2 m_{\mathrm{P}} - \mathrm{j}\omega c_{\mathrm{P3}} - \boldsymbol{R}_2 z_{\mathrm{F11}})\boldsymbol{w}_{2\mathrm{B}}^{-} + \boldsymbol{R}_2 z_{\mathrm{F12}}\boldsymbol{w}_{2\mathrm{B}}^{-}\boldsymbol{e}_{2\mathrm{B}}^{-}(l_{2\mathrm{B}}),$$
$$\mathbf{\Lambda}_{13} = \boldsymbol{R}_2 z_{\mathrm{F13}}\boldsymbol{w}_{2\mathrm{M}}^{+}\boldsymbol{e}_{2\mathrm{M}}^{+}(l_{2\mathrm{B}} + l_{2\mathrm{M}}),$$
$$\mathbf{\Lambda}_{14} = \boldsymbol{R}_2 z_{\mathrm{F13}}\boldsymbol{w}_{2\mathrm{M}}^{-}\boldsymbol{e}_{2\mathrm{M}}^{-}(l_{2\mathrm{B}} + l_{2\mathrm{M}}),$$
$$\mathbf{\Lambda}_{15} = \boldsymbol{R}_2 z_{\mathrm{F14}}\boldsymbol{w}_{2\mathrm{F}}^{+}\boldsymbol{e}_{2\mathrm{F}}^{+}(L_2),$$
$$\mathbf{\Lambda}_{16} = \boldsymbol{R}_2 z_{\mathrm{F14}}\boldsymbol{w}_{2\mathrm{F}}^{-}\boldsymbol{e}_{2\mathrm{F}}^{-}(L_2),$$
$$\mathbf{\Lambda}_{21} = \boldsymbol{w}_{2\mathrm{B}}^{+}\boldsymbol{e}_{2\mathrm{B}}^{+}(l_{2\mathrm{B}}),$$
$$\mathbf{\Lambda}_{22} = \boldsymbol{w}_{2\mathrm{B}}^{-}\boldsymbol{e}_{2\mathrm{B}}^{-}(l_{2\mathrm{B}}),$$
$$\mathbf{\Lambda}_{23} = -\boldsymbol{w}_{2\mathrm{M}}^{+}\boldsymbol{e}_{2\mathrm{M}}^{+}(l_{2\mathrm{B}}),$$
$$\mathbf{\Lambda}_{24} = -\boldsymbol{w}_{2\mathrm{M}}^{-}\boldsymbol{e}_{2\mathrm{M}}^{-}(l_{2\mathrm{B}}),$$
$$\mathbf{\Lambda}_{31} = \boldsymbol{f}_{2\mathrm{B}}^{+}\boldsymbol{e}_{2\mathrm{B}}^{+}(l_{2\mathrm{B}}) - \boldsymbol{R}_2 z_{\mathrm{F21}}\boldsymbol{w}_{2\mathrm{B}}^{+} - \boldsymbol{R}_2 z_{\mathrm{F22}}\boldsymbol{w}_{2\mathrm{B}}^{+}\boldsymbol{e}_{2\mathrm{B}}^{+}(l_{2\mathrm{B}}),$$
$$\mathbf{\Lambda}_{32} = \boldsymbol{f}_{2\mathrm{B}}^{-}\boldsymbol{e}_{2\mathrm{B}}^{-}(l_{2\mathrm{B}}) - \boldsymbol{R}_2 z_{\mathrm{F21}}\boldsymbol{w}_{2\mathrm{B}}^{-} - \boldsymbol{R}_2 z_{\mathrm{F22}}\boldsymbol{w}_{2\mathrm{B}}^{-}\boldsymbol{e}_{2\mathrm{B}}^{-}(l_{2\mathrm{B}}),$$
$$\mathbf{\Lambda}_{33} = -\boldsymbol{f}_{2\mathrm{M}}^{+}\boldsymbol{e}_{2\mathrm{M}}^{+}(l_{2\mathrm{B}}) - \boldsymbol{R}_2 z_{\mathrm{F23}}\boldsymbol{w}_{2\mathrm{M}}^{+}e_{2\mathrm{M}}^{+}(l_{2\mathrm{B}} + l_{2\mathrm{M}}),$$
$$\mathbf{\Lambda}_{34} = -\boldsymbol{f}_{2\mathrm{M}}^{-}\boldsymbol{e}_{2\mathrm{M}}^{-}(l_{2\mathrm{B}}) - \boldsymbol{R}_2 z_{\mathrm{F23}}\boldsymbol{w}_{2\mathrm{M}}^{-}\boldsymbol{e}_{2\mathrm{M}}^{-}(l_{2\mathrm{B}} + l_{2\mathrm{M}}),$$
$$\mathbf{\Lambda}_{35} = -\boldsymbol{R}_2 z_{\mathrm{F24}}\boldsymbol{w}_{2\mathrm{F}}^{+}\boldsymbol{e}_{2\mathrm{F}}^{+}(L_2),$$

$$
\begin{aligned}
\boldsymbol{\Lambda}_{36} &= -\boldsymbol{R}_2 z_{\mathrm{F}24} \boldsymbol{w}^{-}_{2\mathrm{F}} \boldsymbol{e}^{-}_{2\mathrm{F}}(L_2),\\
\boldsymbol{\Lambda}_{43} &= \boldsymbol{w}^{+}_{2\mathrm{M}} \boldsymbol{e}^{+}_{2\mathrm{M}}(l_{2\mathrm{B}} + l_{2\mathrm{M}}),\\
\boldsymbol{\Lambda}_{44} &= \boldsymbol{w}^{-}_{2\mathrm{M}} \boldsymbol{e}^{-}_{2\mathrm{M}}(l_{2\mathrm{B}} + l_{2\mathrm{M}}),\\
\Lambda_{45} &= -\boldsymbol{w}^{+}_{2\mathrm{F}} \boldsymbol{e}^{+}_{2\mathrm{F}}(l_{2\mathrm{B}} + l_{2\mathrm{M}}),\\
\boldsymbol{\Lambda}_{46} &= -\boldsymbol{w}^{-}_{2\mathrm{F}} \boldsymbol{e}^{-}_{2\mathrm{F}}(l_{2\mathrm{B}} + l_{2\mathrm{M}}),\\
\boldsymbol{\Lambda}_{51} &= -\boldsymbol{R}_2 \big[z_{\mathrm{F}31} \boldsymbol{w}^{+}_{2\mathrm{B}} + z_{\mathrm{F}32} \boldsymbol{w}^{+}_{2\mathrm{B}} \boldsymbol{e}^{+}_{2\mathrm{B}}(l_{2\mathrm{B}}) \big],\\
\boldsymbol{\Lambda}_{52} &= -\boldsymbol{R}_2 [z_{\mathrm{F}31} \boldsymbol{w}^{-}_{2\mathrm{B}} + z_{\mathrm{F}32} \boldsymbol{w}^{-}_{2\mathrm{B}} \boldsymbol{e}^{-}_{2\mathrm{B}}(l_{2\mathrm{B}})],\\
\boldsymbol{\Lambda}_{53} &= (\boldsymbol{f}^{+}_{2\mathrm{M}} - \boldsymbol{R}_2 z_{\mathrm{F}33} \boldsymbol{w}^{+}_{2\mathrm{M}}) \boldsymbol{e}^{+}_{2\mathrm{M}}(l_{2\mathrm{B}} + l_{2\mathrm{M}}),\\
\boldsymbol{\Lambda}_{54} &= (\boldsymbol{f}^{-}_{2\mathrm{M}} - \boldsymbol{R}_2 z_{\mathrm{F}33} \boldsymbol{w}^{-}_{2\mathrm{M}}) \boldsymbol{e}^{-}_{2\mathrm{M}}(l_{2\mathrm{B}} + l_{2\mathrm{M}}),\\
\boldsymbol{\Lambda}_{55} &= -\boldsymbol{f}^{+}_{2\mathrm{F}} \boldsymbol{e}^{+}_{2\mathrm{F}}(l_{2\mathrm{B}} + l_{2\mathrm{M}}) - \boldsymbol{R}_2 z_{\mathrm{F}34} \boldsymbol{w}^{+}_{2\mathrm{F}} \boldsymbol{e}^{+}_{2\mathrm{F}}(L_2),\\
\boldsymbol{\Lambda}_{56} &= -\boldsymbol{f}^{-}_{2\mathrm{F}} \boldsymbol{e}^{-}_{2\mathrm{F}}(l_{2\mathrm{B}} + l_{2\mathrm{M}}) - \boldsymbol{R}_2 z_{\mathrm{F}34} \boldsymbol{w}^{-}_{2\mathrm{F}} \boldsymbol{e}^{-}_{2\mathrm{F}}(L_2),\\
\boldsymbol{\Lambda}_{61} &= -\boldsymbol{R}_2 \big[z_{\mathrm{F}41} \boldsymbol{w}^{+}_{2\mathrm{B}} + z_{\mathrm{F}42} \boldsymbol{w}^{+}_{2\mathrm{B}} \boldsymbol{e}^{+}_{2\mathrm{B}}(l_{2\mathrm{B}}) \big],\\
\boldsymbol{\Lambda}_{62} &= -\boldsymbol{R}_2 [z_{\mathrm{F}41} \boldsymbol{w}^{-}_{2\mathrm{B}} + z_{\mathrm{F}42} \boldsymbol{w}^{-}_{2\mathrm{B}} \boldsymbol{e}^{-}_{2\mathrm{B}}(l_{2\mathrm{B}})],\\
\boldsymbol{\Lambda}_{63} &= -\boldsymbol{R}_2 z_{\mathrm{F}43} \boldsymbol{w}^{+}_{2\mathrm{M}} \boldsymbol{e}^{+}_{2\mathrm{M}}(l_{2\mathrm{B}} + l_{2\mathrm{M}}),\\
\boldsymbol{\Lambda}_{64} &= -\boldsymbol{R}_2 z_{\mathrm{F}43} \boldsymbol{w}^{-}_{2\mathrm{M}} \boldsymbol{e}^{-}_{2\mathrm{M}}(l_{2\mathrm{B}} + l_{2\mathrm{M}}),\\
\boldsymbol{\Lambda}_{65} &= \boldsymbol{f}^{+}_{2\mathrm{F}} \boldsymbol{e}^{+}_{2\mathrm{F}}(L_2) - R_2 z_{\mathrm{F}44} \boldsymbol{w}^{+}_{2\mathrm{F}} \boldsymbol{e}^{+}_{2\mathrm{F}}(L_2),\\
\boldsymbol{\Lambda}_{66} &= \boldsymbol{f}^{-}_{2\mathrm{F}} \boldsymbol{e}^{-}_{2\mathrm{F}}(L_2) - R_2 z_{\mathrm{F}44} \boldsymbol{w}^{-}_{2\mathrm{F}} \boldsymbol{e}^{-}_{2\mathrm{F}}(L_2).
\end{aligned}
$$

When the force and bending moment of the drive shaft on the propeller are zero, the det = 0 is a transcendental equation, so you can solve for an infinite number of free vibration frequencies of the system, namely the natural frequencies of the bending vibration of the system in the frequency domain.

95.2.2 Analysis of Vibration Energy Transfer

Average power input of propeller lateral excitation to shafting vibration:

$$
P_{1\mathrm{H}} = \frac{\omega}{2\pi} \int_0^{2\pi/\omega} \mathrm{Re}\left\{ \tilde{F}_{\mathrm{P}} \right\} \cdot \mathrm{Re}\left\{ -\dot{\tilde{w}}_{\mathrm{P}} \right\} \mathrm{d}t = \frac{1}{2} \mathrm{Re}\left\{ \underline{\tilde{F}}_{\mathrm{P}} \cdot (-\mathrm{j}\omega W_{\mathrm{P}})^{*} \right\}
$$

$$
= \frac{1}{2} \mathrm{Re}\left\{ \underline{\tilde{F}}_{\mathrm{P}} \cdot \mathrm{j}\omega W^{*}_{2}(0, \omega) \right\} \tag{95.7}
$$

Introduce the concepts of complex stiffness and complex wave number, and the transmitted power flow at the connection between propeller and shafting system is as follows:

$$P_{\mathrm{EI}} = \frac{\omega}{2\pi}\int_0^{2\pi/\omega}\Big[\mathrm{Re}\big\{(EI)_{2\mathrm{B}}\tilde{w}_{2\mathrm{B},xx}(0,t)\big\}\cdot\mathrm{Re}\Big\{-\dot{\tilde{w}}_{2\mathrm{B},x}(0,t)\Big\} + \mathrm{Re}\big\{(EI)_{2\mathrm{B}}\tilde{w}_{2\mathrm{B},xxx}(0,t)\big\}\cdot\mathrm{Re}\Big\{\dot{\tilde{w}}_{2\mathrm{B}}(0,t)\Big\}\Big]\mathrm{d}t \tag{95.8}$$

The average power dissipated by fluid damping in the process of propeller bending vibration with shafting:

$$P_{\mathrm{Cp2}} + P_{\mathrm{Cp3}} = 0.5\omega^2\big(c_{\mathrm{P2}}\big|l_{\mathrm{MB}}|^2\big| - \mathrm{j}A_{\mathrm{MB}} - B_{\mathrm{MB}} + \mathrm{j}C_{\mathrm{MB}} + D_{\mathrm{MB}}\big|^2 + c_{\mathrm{P3}}\big|A_{\mathrm{MB}} + B_{\mathrm{MB}} + C_{\mathrm{MB}} + D_{\mathrm{MB}}|^2\big|\big) \tag{95.9}$$

c_{P2} and c_{P3} are the damping coefficients when the blades move the seawater.

Assume that the excitation force and bending moment of aft stern bearing on the hull is $\tilde{F}_{3\mathrm{H}}$ and $\tilde{M}_{3\mathrm{H}}$, and the average power is $P_{13\mathrm{H}}$ and $P_{23\mathrm{H}}$:

$P_{13\mathrm{H}} = \frac{1}{2}\mathrm{Re}\left\{\mathrm{j}\omega\alpha_{32}^{\mathrm{H}}\mathbf{W}_{32}^{\mathrm{H}}\mathbf{H}_{11}^{\mathrm{H}}\cdot\begin{bmatrix}1&0\\0&0\end{bmatrix}\cdot\mathbf{Z}_{11}\mathbf{W}_{32}\alpha_{32}\right\}$, $P_{23\mathrm{H}} = \frac{1}{2}\mathrm{Re}\left\{\mathrm{j}\omega\alpha_{32}^{\mathrm{H}}\mathbf{W}_{32}^{\mathrm{H}}\mathbf{H}_{11}^{\mathrm{H}}\cdot\begin{bmatrix}0&0\\0&1\end{bmatrix}\cdot\mathbf{Z}_{11}\mathbf{W}_{32}\alpha_{32}\right\}$.

Then the total average power input transmitted from the aft bearing to the hull is: $P_{3\mathrm{H}} = P_{13\mathrm{H}} + P_{23\mathrm{H}}$. Similarly, the total average power input of stern front bearing, stern middle bearing and thrust bearing transmitted to the hull is $P_{2\mathrm{H}} = P_{12\mathrm{H}} + P_{22\mathrm{H}}$,$P_{1\mathrm{H}} = P_{11\mathrm{H}} + P_{21\mathrm{H}}$,$P_{\mathrm{TH}} = P_{1\mathrm{TH}} + P_{2\mathrm{TH}}$, and the sum of the power flow of each bearing seat and hull structure is $P_{\mathrm{SUM}} = P_{3\mathrm{H}} + P_{2\mathrm{H}} + P_{1\mathrm{H}} + P_{\mathrm{TH}}$.

Set the energy density of each sub-shaft bending vibration in unit volume as $\langle T_{2\mathrm{B}}(x,\omega)\rangle$, $\langle T_{2\mathrm{B+2M}}(x,\omega)\rangle$; and $\langle T_{\mathrm{L2}}(x,\omega)\rangle$, and the energy density of the bending deformation potential energy as $\langle V_{2\mathrm{B}}(x,\omega)\rangle$,$\langle V_{2\mathrm{B+2M}}(x,\omega)\rangle$; and $\langle V_{\mathrm{L2}}(x,\omega)\rangle$.

Total bending vibration energy:

$$\begin{aligned}\left\langle\bar{E}(\omega)\right\rangle &= \left\langle\bar{E}_{2\mathrm{B}}(\omega)\right\rangle + \left\langle\bar{E}_{2\mathrm{B+2M}}(\omega)\right\rangle + \left\langle\bar{E}_{\mathrm{L2}}(\omega)\right\rangle \\ &= \int_0^{l_{2\mathrm{B}}}\langle E_{2B}(x,\omega)\rangle\mathrm{d}x + \int_{l_{2\mathrm{B}}}^{l_{2\mathrm{B}}+l_{2\mathrm{M}}}\langle E_{2\mathrm{B+2M}}(x,\omega)\rangle\mathrm{d}x \\ &\quad + \int_{l_{2\mathrm{B}}+l_{2\mathrm{M}}}^{L_2}\langle E_{\mathrm{L2}}(x,\omega)\rangle\mathrm{d}x\end{aligned} \tag{95.10}$$

Average vibration energy of propeller:

$$\langle T_{\mathrm{P}}\rangle = \frac{\omega}{4\pi}\int_0^{2\pi/\omega} m_{\mathrm{P}}\Big(\mathrm{Re}\Big\{\dot{\tilde{w}}_{\mathrm{P}}\Big\}\Big)^2\mathrm{d}t + \frac{\omega}{4\pi}\int_0^{2\pi/\omega} J_{\mathrm{P}}\Big(\mathrm{Re}\Big\{\dot{\tilde{\varphi}}_{\mathrm{P}}\Big\}\Big)^2\mathrm{d}t \tag{95.11}$$

95.3 Calculation of Bearing Lubrication and Liquid Film Stiffness

The pressure changes caused by unit displacement of radial and thrust bearings were obtained by simulating small displacement disturbance based on ANSYS, then obtain the liquid film stiffness of the bearing.

95.3.1 Boundary Conditions and Flow Conditions

Based on the related mathematical theory of hydrodynamic lubrication, then introduce the Reynolds equation [7]. The boundary condition is $p = p_0$, $\partial p / \partial \psi = 0$ [8, 9] . The Reynolds number Re = ρvd/μ can indicate that the fluid has a critical transition from laminar flow to turbulent flow.d is a characteristic length, μ is the hydrodynamic viscosity) Reynolds number is the basis for judging the flow characteristics. In pipe flow, the flow with Reynolds number less than 2300 is laminar flow, the flow with Reynolds number equal to 2300–4000 is a transitional state, and when it is greater than 4000, it is turbulent flow [10]. Take fluid density 0.95×10^{-3} kg/m^3, dynamic viscosity coefficient 0.047 Pa s, speed 40 rad/s, characteristic length 1×10^{-4} m, and calculate Re ≅ 13.9, which is much less than 2300 Reynolds number, so the flow state of lubricating oil in the bearing gap is laminar flow.

95.3.2 Stiffness Characteristic Calculation of Tilting Tile Bearing

Define the length between the oil outlet and the oil inlet of the bearing bush as D, the length between the fixed fulcrum and the oil inlet is d, set the tilting pad bearing clearance ratio as c_ζ, the axial thickness of the liquid film at the bearing pad gap is 10 mm, and the standard oil film clearance on the side of the sector-shaped bearing pad is 0.1 mm, define the gap between the front thrust plate and the stepped shaft as $c_{f,}$ and the gap between the rear thrust plate and the stepped shaft as $c_{b.}$ Set 5 rad/s, 10 rad/s, 15 rad/s, 20 rad/s, 25 rad/s five speed working conditions, c_f select a series of values between 0.04–0.16.

Responding to different c_f can be calculated. Based on FLUENT simulation, the bearing capacity co draw the scatter trend graph of the data to get the bearing oil film bearing capacity-clearance-speed relationship graph. The slope of each linear equation is the lubricating oil film stiffness K_L of the tilting pad sector thrust bearing at the corresponding speed. The statistics are shown in Table 95.1.

The calculated results are consistent with the order of magnitude of oil film stiffness in relevant literature [11, 12], which proves that the calculated results are effective.

Table 95.1 Tilting pad thrust bearing oil film rigidity table

Rotating speed/(rad/s)	5	10	15	20	25
Stiffness/ N/m × 10^8	0.346	0.682	1.06	1.41	1.74

Table 95.2 Some calculation parameters of stern front bearing

Name	The radius of the bearing bush	The radius of the front stern shaft	The axial width	Gap width
The numerical/mm	67.65	67.5	325.5	0.1

Table 95.3 Stiffness of bearing liquid film of stern front, stern, and stern under different working conditions

Rotating speed/rad·s^{-1}	5	10	15	20	25	40
K1/N m^{-1} × 10^8	1.8	2.62	3.5	4.38	5.27	7.91
K2/N m^{-1} × 10^8	1.67	2.8	3.15	4.65	5.74	8.58
K3/N m^{-1} × 10^8	3.24	5.11	6.72	9.37	11.5	18.3

95.3.3 Stiffness Characteristic Calculation of Radial Bearings

The structure of the three radial sliding bearings is similar, the lubrication principle and the calculation method of the liquid film stiffness are the same, so only the calculation process of the stern front bearing is listed here.

Pre-processing is performed based on the stern bearing parameters in Table 95.2 and Solidworks software. In addition to the five working conditions of 3.2 knots of shaft speed, a shaft speed of 40 rad/s is added to simulate the navigating conditions of the ship, and the air separation pressure is set to 7750 Pa.

Using the same calculation method, the speed-liquid film stiffness relationship of the stern intermediate bearing and the stern bearing can be obtained. K_1, K_2, and K_3 are used to represent the liquid film stiffness of the front, middle, and rear stern bearings respectively as shown in Table 95.3.

95.4 Relationship Between Fluid Film Stiffness of Plain Bearings and Energy Transfer of Bending Vibration in Shafting System

Combining the above simulation calculation results reflecting the dynamic characteristics of radial sliding bearings with the calculation model of shaft bending vibration energy transfer, then perform simulation calculations in three working conditions

(speed 5 rad/s, 15 rad/s and 25 rad/s) to analyze the influence of the stiffness characteristics of the front, middle and rear radial bearings and tilting pad support bearings on the average power input and dissipation of the shafting bending vibration. Substitute the parameters in Tables 95.1, 95.2 and 95.3 into MATLAB, and then get the energy dissipation diagram of bending vibration in the transmission path of propeller-shaft-bearing-hull, as shown in Figs. 95.3, 95.4, 95.5 and 95.6.

It can be seen from Fig. 95.3 that while the increase in speed leads to an increase in the stiffness of the bearing liquid film, it also causes the natural frequency to shift to the right. At the same time, the energy dissipation effect in the high frequency range is also increased, but the dissipation effect is not obvious. It can be seen from Fig. 95.4 that in the low-frequency region, a higher rotation speed can significantly increase the resonance frequency of the shaft system excited by the propeller; the impact of energy dissipation in the high-frequency region is difficult to distinguish, and the effect is not obvious. It can be seen from Fig. 95.5 that When the stiffness of the liquid film of each bearing rises because of the increase in speed, the resonance frequency in the low-frequency resonance region has an exponential increase trend,

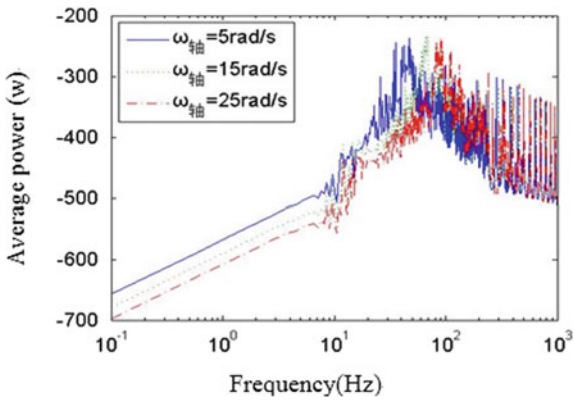

Fig. 95.3 Average power dissipation of shafting bending vibration

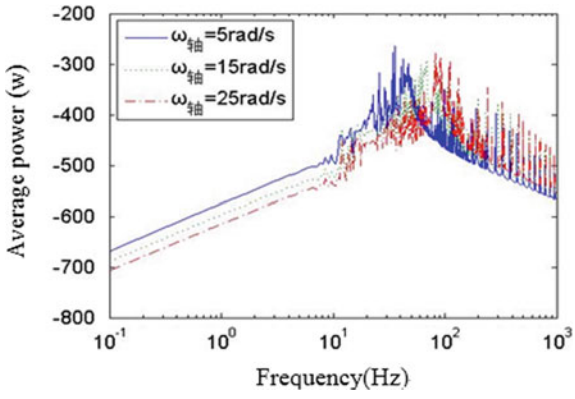

Fig. 95.4 Power flow input at the paddle shaft connection

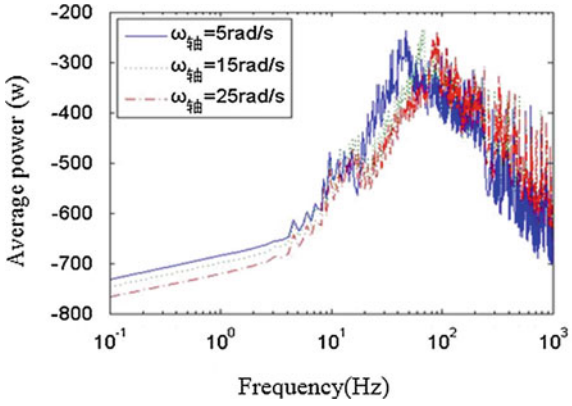

Fig. 95.5 Average energy input from each to the hull

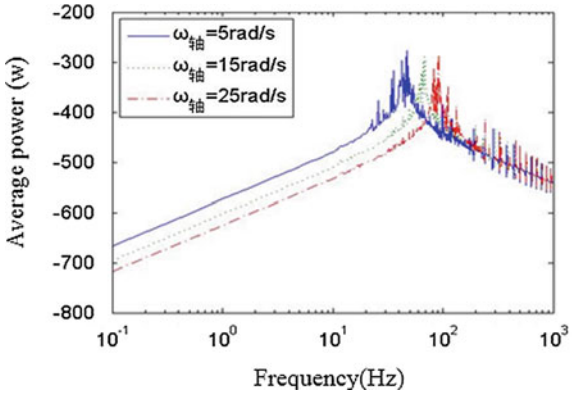

Fig. 95.6 Mean value of propeller vibration bearing energy dissipation

The average energy input in the medium and high frequency region will decrease rapidly as the stiffness of the liquid film of each bearing increases (The increase in the stiffness of the bearing liquid film is proportional to the shaft speed). Figures 95.3, 95.4, 95.5 and 95.6 have a common character: when the liquid film stiffness of each sliding bearing increases due to the increase of speed, the natural frequency in the low-frequency region moves significantly to the right. Figure 95.6 also shows that the increase of rotating speed and bearing liquid film stiffness has a certain effect on vibration energy transfer and dissipation in the low frequency region, but it has no obvious effect on the vibration energy transfer and dissipation in the middle and high frequency region.

In summary, the stiffness of the bearing liquid film is proportional to the speed of the drive shaft and inversely proportional to the main resonance peak frequency; The stiffness of the bearing liquid film is proportional to the dissipation ability of low frequency vibration energy transmission, while has little influence on the dissipation process of high frequency vibration energy transmission.

95.5 Conclusions

Based on the general structure of the ship's propulsion shafting, this paper built a theoretical model of the bending vibration of the ship-shaft coupling system and the average energy input calculation model in Sect. 95.2. In Sect. 95.3, it simulates and calculates the oil film stiffness of three radial bearings and tilting pad thrust bearings of the stern drive shaft in 6 different speed conditions. In Sect. 95.4, the calculation results of Sect. 95.2 are substituted into the average power calculation model of bending vibration for simulation calculation and effect analysis. According to the research, When the speed decreases, the stiffness of the liquid film of each bearing decreases, at the same time, the frequency of each main resonance peak decreases, and the vibration energy of the lower frequency band is amplified. The effect of the change of bearing liquid film stiffness at different speeds on the energy transfer of shaft bending vibration is mainly concentrated in the low-frequency area, while the effect on the high-frequency area is not obvious. This conclusion provides a theoretical basis and research method for the study of shafting noise radiation.

References

1. Wasilczuk, M., Wasilczuk, F.: Combined thrust radial bearing of a submarine main shaft—design and analysis of failure. Eng. Failure Anal. **115** (2020)
2. Litwin, W.: Influence of main design parameters of ship propeller shaft water-lubricated bearings on their properties. Polish Maritime Res. **17**(4), 39–45 (2010)
3. Litwin, W.: Water: an extraordinary, ordinary lubrication liquid. In: Influence of Water Salinity, Pressure and Temperature on Water Lubricated Bearings Properties (2010)
4. Wang, R., Zhu, H., Yan, X., et al.: Influence of oil film thickness on shafting vibration of ship sliding bearing. Lubr. Eng. **41**(07), 38–42 (2016)
5. Litwin, W.: Influence of local bush wear on water lubricated sliding bearing load carrying capacity. Tribol. Int. **103**, 352–358 (2016)
6. Tiwari, R., Chakravarthy, V.: Simultaneous identification of residual unbalances and bearing dynamic parameters from impulse responses of rotor–bearing systems. Mech. Syst. Signal Process. **20**(7), 1590–1614 (2006)
7. Kini, M.V., Pai, R.S., Rao, D.S., et al.: Effect of groove location on the dynamic characteristics of multiple axial groove water lubricated journal bearing. World Acad. Sci. Eng. Technol. **60** (2013)
8. Wang, L.: Study on Wall Ship and Cavitation Mechanism of a High Speed Journal Bearing. Shan Dong University (2012)
9. Shao, K., Liu, C.W., Bi, F.R., et al.: Analysis of hydrodynamic loads on performance characteristics of engine main bearings. Proc. Inst. Mech. Eng., Part J. J. Eng. Tribol **229**(6), 667–676 (2015)
10. Yang, G.: Research on the Influence of Bearings Lubrication to Shafting Vibration. Harbin Engineering University (2015)
11. Li, Z., et al.: Study on coupling effect of crankshaft lubrication and bending vibration in diesel engine. Lubrication Eng. **45**(1), 129–134 (2020). ISSN 0254–0150
12. Wong, H.C., Umehara, N., Kato, K.: The effect of surface roughness on friction of ceramics sliding in water. Wear **218**(2), 237–243 (1998)
13. Opitz, A., Ahmed, I.U., Schaefer, J.A., et al.: Friction of thin water films: a nanotribological study. Surf. Sci. **504**(1–3), 199–207 (2002)

Shuqing Liu, born in 1998, is currently a master candidate student at Shandong University, China. He received his bachelor degree from Huazhong agriculture University, China, in 2020. His research interests include Vibration and noise of the hull.

Rui Huo, born in 1967, is currently a professor and Ph.D. candidate supervisor at Shandong University, China. He received his Ph.D. degree from Shandong University of Technology, China, in 1998. His research interests include dynamics of mechanical systems and vibration and noise control.

Yuanbo Li, born in 1986, is currently a master candidate student at Shandong University, China. He received his master degree from Shandong University, China, in 2021. His research interests include active noise control.

Chuangye Li, born in 1986, He received his master degree from Shandong University, China, in 2019. His research interests include Shaft vibration.